

NASA TECHNICAL NOTE



NASA TN D-3202

c.1

NASA TN D-3202

LOAN COPY: RETU  
AGWL (VILL  
KIRTLAND AFB, N



# SELECTED MECHANICAL AND PHYSICAL PROPERTIES OF BORON FILAMENTS

*by Harvey W. Herring  
Langley Research Center  
Langley Station, Hampton, Va.*



TECH LIBRARY KAFB, NM



0079877

NASA TN D-3202

SELECTED MECHANICAL AND PHYSICAL PROPERTIES  
OF BORON FILAMENTS

By Harvey W. Herring

Langley Research Center  
Langley Station, Hampton, Va.

NATIONAL AERONAUTICS AND SPACE ADMINISTRATION

---

For sale by the Clearinghouse for Federal Scientific and Technical Information  
Springfield, Virginia 22151 - Price \$2.00

## SELECTED MECHANICAL AND PHYSICAL PROPERTIES

### OF BORON FILAMENTS

By Harvey W. Herring  
Langley Research Center

#### SUMMARY

Results are presented from an investigation to characterize boron filaments with respect to selected mechanical and physical properties. The investigation of 12 different filaments included examination by metallographic techniques and the determination of mechanical properties over the temperature range from room temperature to 2500° F (1644° K) in argon, air, and vacuum.

The study was primarily concerned with the properties of individual boron filaments produced by the deposition of boron on the surface of a fine tungsten substrate wire from a vapor composed of hydrogen and a boron halide compound. These filaments exhibited an average room-temperature strength of 350 ksi (2.42 GN/m<sup>2</sup>) and retained approximately two-thirds of this strength at temperatures up to 2000° F (1366° K). The range of scatter among individual tensile strength values was generally equal to the mean value of strength. An average Young's modulus value of  $60 \times 10^3$  ksi (414 GN/m<sup>2</sup>) was recorded.

#### INTRODUCTION

Filaments made of boron appear promising for use in certain reinforced composite material applications where increased stiffness and elevated-temperature strength are desirable. Boron filaments in a form suitable for structural applications were first reported in the literature in 1960 (ref. 1). Since that time, several reports concerning the development and characterization of high-modulus filaments, particularly those made of boron, have become available (for example, refs. 2 and 3).

To explore the potential of boron filaments for possible use in composite structures, a study was made at the NASA Langley Research Center to determine certain mechanical and physical properties. Results from 12 different filaments were obtained. The investigation included the determination of filament tensile strength over the temperature range from room temperature to 2500° F (1644° K) in both air and inert atmospheres and a study of the effect of environmental exposure at elevated temperature on filament strength. The elastic moduli in tension of the various filaments were also determined. A series of tensile tests was conducted to determine the effect of specimen gage length on

filament strength. Results of these tests are presented along with a statistical analysis of some of the mechanical property data that exhibit typical scatter.

The units used for the physical quantities defined in this paper are given in both U.S. Customary Units and the International System of Units (SI) (ref. 4). Appendix A presents factors relating these two systems of units.

## TEST SPECIMENS

### General Characteristics of Boron Filaments

A schematic representation of a typical boron filament is shown in figure 1. Boron filaments are made by a process in which elemental boron is

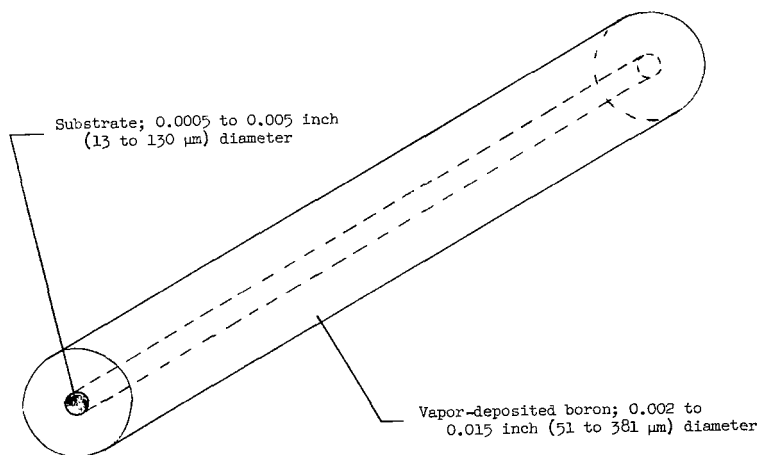


Figure 1.- Schematic representation of a boron filament.

deposited from a vapor onto the surface of a fine metallic substrate wire which is resistance heated and moves continuously through the deposition chamber. Varying properties may be produced by changing the substrate material, the composition of the chemical compound(s) comprising the vapor, the temperature of the substrate, and the velocity with which the substrate progresses through the reaction chamber. The filaments involved in this study are listed in table I, and are separated into two general categories: halide-process boron filaments and organometallic-process boron

filaments. The filaments are coded by letter to permit easy reference to them throughout the remainder of the text. Manufacturers are also listed in table I. The filaments investigated herein are not necessarily the best obtainable from the manufacturers listed, and the list of manufacturers is included only for general information.

### Halide-Process Boron Filaments

The halide-process boron filaments are so designated because they are produced by the hydrogen reduction of a boron halide such as boron trichloride ( $\text{BCl}_3$ ) or boron tribromide ( $\text{BBr}_3$ ) at the surface of a substrate wire (in this study, tungsten). The temperature associated with the process is in the neighborhood of  $2000^\circ\text{F}$  ( $1366^\circ\text{K}$ ). The reaction is of sufficient duration for all

the tungsten and some of the deposited boron to react to form a core of tungsten borides. A general description of the halide-reduction process for the manufacture of boron filaments may be found in references 1, 5, 6, and 7. The diameter of halide-process boron filaments may be varied by adjusting the deposition parameters. In the present study the diameters of halide-process filaments are from 0.0017 to 0.0047 inch (43 to 120  $\mu\text{m}$ ). The initial substrate diameter in each case is 0.0005 inch (13  $\mu\text{m}$ ).

### Organometallic Process Boron Filaments

The presence of tungsten wire in the halide-process boron filaments is undesirable for two reasons: First, it is expensive; and second, it imposes a weight penalty on the filament. Accordingly, a brief study was made to investigate the possibility of using lighter and cheaper substrate materials in the production of boron filaments. The most likely candidate was aluminum wire, and for this reason, it was necessary to make use of a vapor deposition process which would be operative at a temperature below the melting point of aluminum (1220° F (933° K)). The process chosen involved the deposition of boron from the pyrolysis of a boron organometallic compound such as triethyl boron ((C<sub>2</sub>H<sub>5</sub>)<sub>3</sub>B), or one of the borane series of hydrides (such as B<sub>2</sub>H<sub>6</sub> or B<sub>5</sub>H<sub>9</sub>). The organometallic-process boron filaments were produced in 12-inch (30.5-cm) lengths under contract to the Langley Research Center. Their diameters ranged from 0.002 to 0.015 inch (51 to 380  $\mu\text{m}$ ). Three substrate materials were investigated: titanium (Ti), tungsten (W), and aluminum (Al); the diameters were 0.001 inch (25  $\mu\text{m}$ ) for each material. The temperatures involved in the organometallic processes were within the range from 600° to 1500° F (589° to 1089° K) and were low enough so that there was essentially no reaction between the substrate and the deposited boron. A general description of the organometallic-vapor-deposition method for producing boron filaments may be found in reference 7.

### TEST PROGRAM

Boron filament specimens were subjected to a series of tests designed to determine the modulus of elasticity in tension; filament tensile-strength tests were also conducted over a range of temperatures. Several filament specimens were examined by metallographic techniques for the purpose of determining microhardness and microstructure.

#### Tensile Tests

Tensile tests of all filament specimens with gage lengths up to 20 inches (0.508 m) were conducted in a screw powered machine. Load (force) was measured by a 50 lbf (222 N) capacity load cell. The measured load was recorded automatically on a strip chart. Full-scale deflection on the chart was adjusted to loads of from 1 to 10 lbf (4.45 to 44.5 N) depending on the diameter of the filament. The sensitivity of the load cells required that they be calibrated

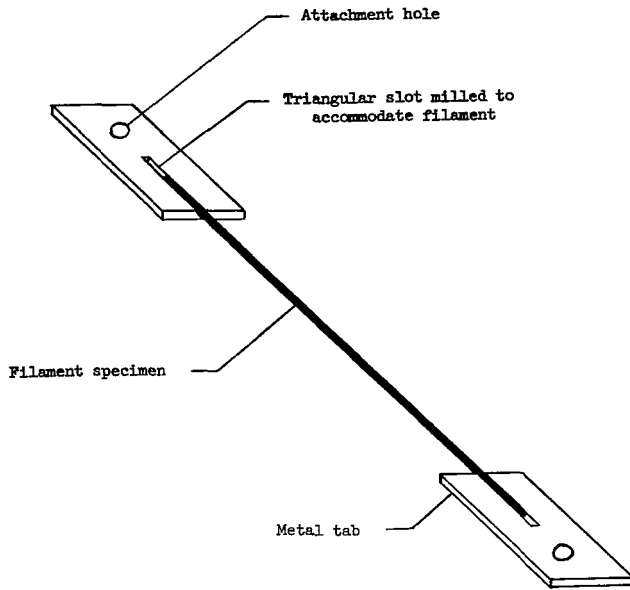
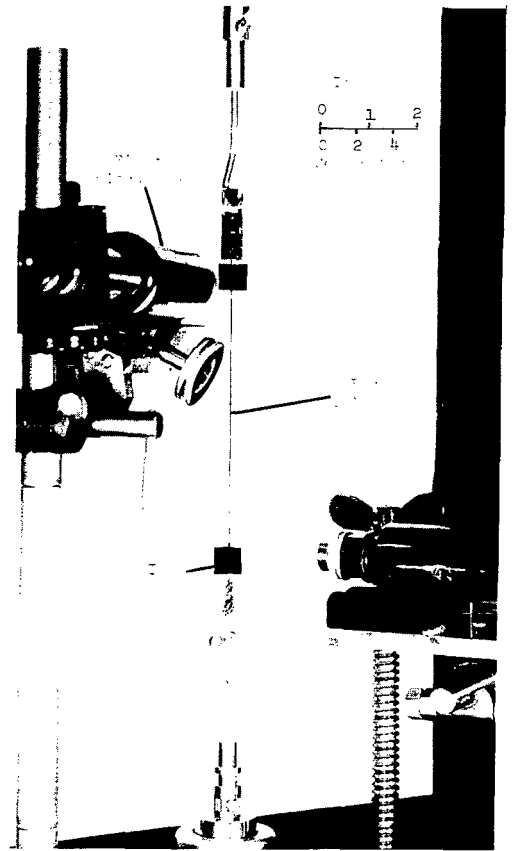


Figure 2.- Filament tensile specimen.

before each test. This calibration was accomplished by the use of weights which are accurate to within 0.01 lbm (4.54 g). A cross-head speed of 0.05 in/min (21  $\mu\text{m/s}$ ) was used for all machine tests. Specimens were mounted in the machine by bonding them to metal tabs at either end (fig. 2) with red sealing wax for room-temperature tests of small-diameter filament specimens. A room-temperature curing epoxy was used as the adhesive for all elevated-temperature tests and for tests of large-diameter filaments the strength of which was sufficiently great to cause slippage in the wax. Specimens with gage lengths in excess of 20 inches (0.5 m) were tested by suspending them from a fixed support in the laboratory. Load (force) was applied by the addition of measured quantities of water to a container which had been affixed to the bottom end of the specimen.

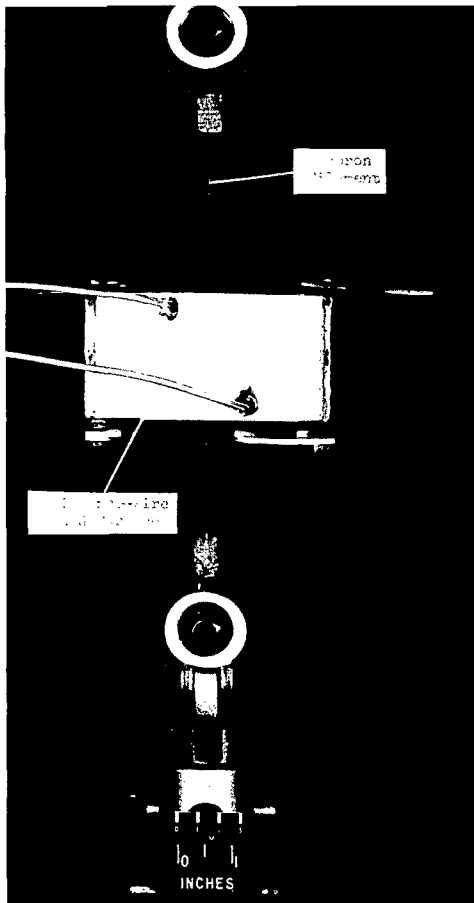
#### Stress-Strain Tests

For the stress-strain tests, specimen elongation during tensile loading was measured with two filar microscopes which are accurate to within 0.0001 inch (2.5  $\mu\text{m}$ ). The microscopes are shown mounted on the testing machine in figure 3. Load (force) was applied to the specimen in increments of from 5 to 20 percent of the ultimate filament strength. After each load increment had been applied, the load was held constant for a few seconds while measurements were made with both the upper and lower microscopes. The lower microscope was used to measure the total downward displacement of the bottom end of the filament specimen, and



L-63-8704.1

Figure 3.- Apparatus for determining Young's modulus of boron filaments.



L-64-8084.1

Figure 4.- Apparatus for elevated-temperature tensile testing of boron filaments.

the upper microscope was used to measure a corresponding displacement of the upper gripping mechanism which might have occurred as a result of the applied load. The microscopes were sighted in on the edges of small strips of masking tape which had been affixed to either end of the specimen. It is believed that any error introduced as a result of slippage of the strips of tape relative to the filament specimen is minimal.

#### Elevated-Temperature Tensile Tests

Elevated-temperature tensile-strength tests were conducted in a platinum-wire wound, closed-tube resistance furnace (fig. 4) capable of being operated with an atmosphere of either air or argon. The test temperature was measured with a chromel-alumel thermocouple inserted into the furnace tube parallel to, and in close proximity with the filament specimen. Tensile tests were conducted both in still air and in 99.995-percent pure argon (dewpoint  $-75^{\circ}$  F ( $222^{\circ}$  K)) flowing at a rate of 10 cubic feet per hour ( $80 \text{ cm}^3/\text{s}$ ). All specimens tested were exposed at temperature for 60 seconds before testing.

#### Tests of Specimens Exposed at

#### Elevated Temperature

Several groups of specimens were tested in tension at room temperature after being exposed at elevated temperature for 15 minutes in air or vacuum. Filaments exposed in air were inserted into an open-tube resistance furnace which had been previously brought to temperature and stabilized. Specimens exposed in vacuum were placed in a similar furnace which was then evacuated, brought to temperature, and held for the required exposure time. Heating and cooling times for the vacuum furnace were 1.0 and 2.5 hours, respectively. The pressure in the furnace was  $1 \times 10^{-5}$  torr ( $1.33 \text{ mN/m}^2$ ) at the exposure temperature.

#### Metallographic Examination

External boron-filament surfaces were photomicrographed without alteration at various magnifications from 25 to 1000. Filament specimens were sectioned for metallographic examination by cutting with either a diamond abrasive wheel or a fine stream of compressed air laden with alumina particles. The sections were further prepared by wet grinding with 600 grit silicon-carbide paper and

then polishing with either 0.1 micron (0.1  $\mu\text{m}$ ) levigated gamma alumina on a rotating microcloth-covered wheel, or 6 micron (6  $\mu\text{m}$ ) diamond paste on a vibrating nylon-covered platform. Microhardness indentations were made with a certified 136° (2.38 rad) diamond pyramid under a 0.1 kgf (0.98 N) load. Load duration was approximately 20 seconds. Indentation diagonals were measured with a filar microscope which had been calibrated with a stage micrometer. Both measurements and calibration were performed at a magnification of 750.

## RESULTS AND DISCUSSION

### Summary of Room-Temperature Tensile Tests

The average tensile strengths of all filament specimens are presented in figure 5. All tests were conducted on 1-inch (2.54-cm) gage-length specimens, where gage length is defined as the length between the two attachment tabs (fig. 2). Filaments A, B, C, D, and E were produced by the halide-reduction process and are significantly stronger than the remainder of the filaments which were produced by organometallic-decomposition processes.

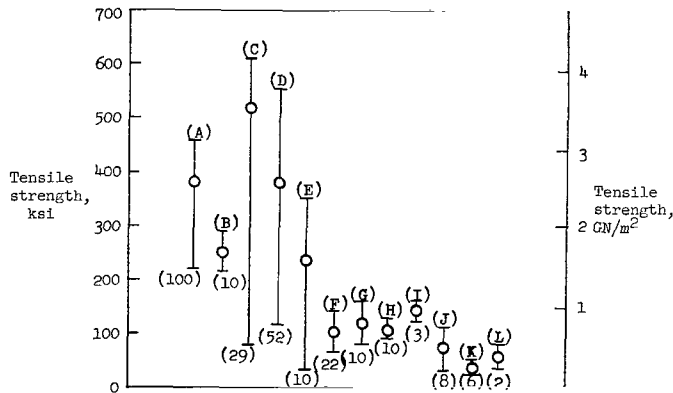


Figure 5.- Average tensile strength of all filaments tested. Gage length, 1 inch (2.54 cm). Letters in parentheses indicate filament type. Numbers in parentheses indicate number of tests upon which each point is based.

The data from all tensile-strength tests of halide-process filaments are presented in table II. The average strength of all the halide-process filaments tested was approximately 350 ksi (2.42 GN/m<sup>2</sup>) compared with an average of 100 ksi (0.69 GN/m<sup>2</sup>) for the strength of the organometallic-process filaments.

### Factors affecting the strength difference among filament types.

There are a number of factors which contribute to the strength differential between the two filament classes. The halide-process filaments were in a much more advanced state of development than were those produced from the organometallic decompositions at the time the tests were conducted. The halide-reduction process for making boron filaments had been advanced to a degree where filaments were being produced on a continuous basis at the rate of thousands of feet (hundreds of meters) per day. The organometallic-process filaments, however, were being produced for the first time in batch reactors capable of only a few 12-inch (30-cm) lengths per day. In addition, control of the reaction temperature associated with vapor deposition from the borane series of compounds was critical. If the temperature varied from within a very limited range, complex boron hydride polymers were formed as a decomposition byproduct and were included in

the deposited boron. Accurate measurement of the reaction temperature was made difficult by the fact that, in the majority of instances, it was so low that the substrate wire was not incandescent. It was necessary to estimate the temperature based on measured power input and estimated losses. In cases where the substrate wire was at red heat, the interior walls of the glass-reaction chamber became coated with the polymeric boron hydrides thus rendering optical temperature measurements unreliable. Finally, the lack of uniformity of the substrate wires was a problem in several instances. When the wires were resistance heated, hot spots developed which adversely affected the boron deposit in those areas. The optimum properties of organometallic-process filaments are probably not represented by the results of this study. It is possible that further development might improve the filaments considerably.

Effect of diameter measurement on filament strength.- The diameter of boron-filament specimens was measured at three or more points along their lengths with a calibrated filar microscope, and the average value was used in stress calculations. The diameter of the filaments obtained from a hand micrometer was found to be approximately 0.0001 inch (2.5  $\mu\text{m}$ ) less than a corresponding microscope reading. As a result, stresses reported herein are somewhat lower than they would have been had the stress calculations been based on the micrometer method of diameter measurement.

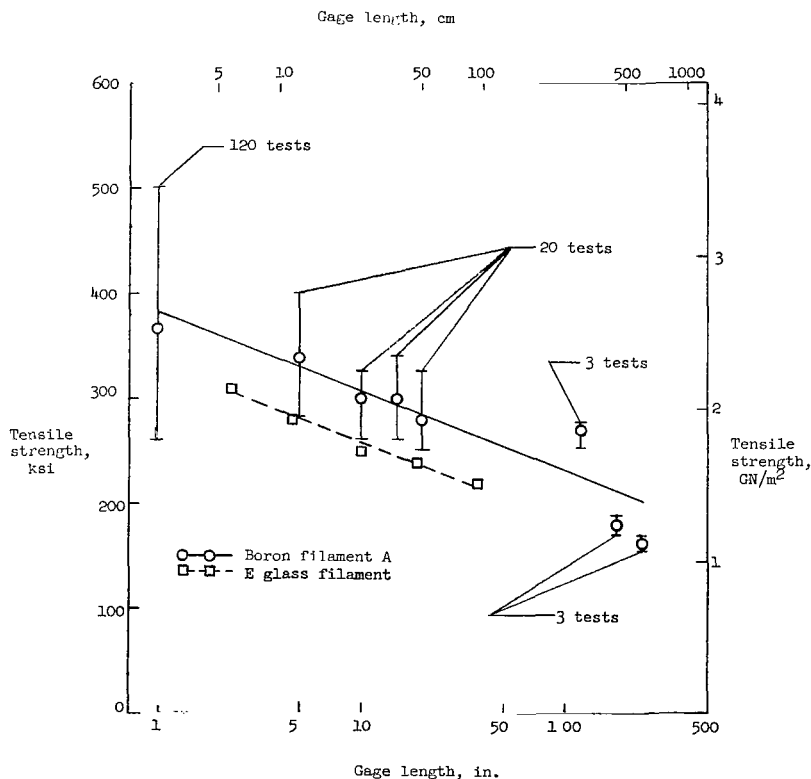


Figure 6.- Effect of gage length on tensile strength of boron filament A. Filament diameter, 0.0018 inch (46  $\mu\text{m}$ ). Similar data for E-glass filament shown for comparison.

Effect of gage length on filament strength.- No evidence of plastic deformation was observed in boron filaments under tension. Therefore, any discontinuity or flaw which exists in a stressed filament is associated with a stress concentration which cannot be relieved by plastic deformation. A particular stress concentration can only result in atomic separation at a stress level which depends on the location, orientation, and severity of the flaw. One effect of this lack of ductility in boron filaments is that tensile strength decreases markedly with increasing gage length. This result is expected since the probability of occurrence of a severe flaw increases as the volume of material increases. Figure 6 shows

the results of a series of tensile tests of boron filament A with specimen gage length varying from 1 to 240 inches (2.54 to 610 cm). A particular group of 120 tests was chosen for this presentation because (of all specimens tested) this was the largest number tested consecutively from a single reel of filament. In figure 6 filament A exhibits behavior which is typical of all halide-process filaments tested. The effect of gage length on the tensile strength of filament A is compared with similar data for E-glass filament (ref. 8) which is brittle, of nearly equal density, and in common use in the fabrication of filament-wound composite structures. Within the comparable range of lengths, the slopes of the two curves are nearly similar and therefore suggest similar occurrence of flaws in both materials.

Problem of scatter.- Another effect of the lack of ductility in boron filaments is that considerable scatter is observed among individual tests in any given property determination.

Many tests are necessary before an average value of a specific property can be predicted with accuracy. Because of a limited supply of filaments, many of the results presented herein are based on a number of experimental determinations which may be less than a statistical sample. However, these results establish a general trend even though the curve may be subject to some changes if larger quantities of filaments were tested - particularly filaments of longer lengths. A statistical analysis of the variation of strength with gage length is presented in appendix B.

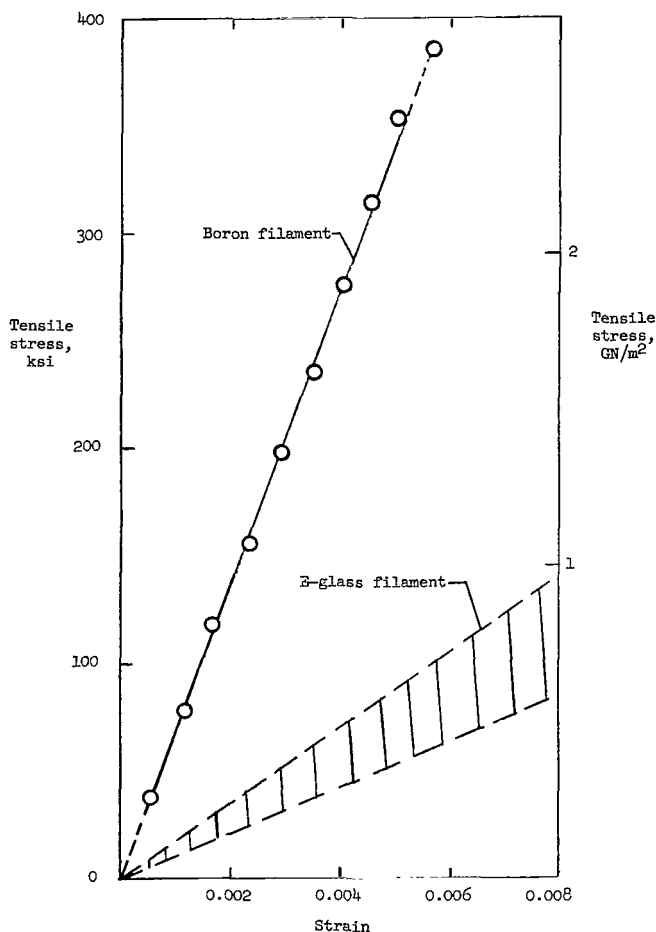


Figure 7.- Typical stress-strain curve for boron filament A. Gage length, 10 inches (25.4 cm). Diameter, 0.0018 inch (46  $\mu$ m). Dashed segments of boron curve represent extrapolations of experimental data.

Young's modulus of boron filaments.- A typical stress-strain curve for boron filament A is shown in figure 7. The range of stress-strain curves for commercially available E-glass filaments is shown for comparison. The dashed portions at either end of the experimental curve represent extrapolations since strain values relative to zero load and at failure were not measured. Average Young's modulus values for all the halide-process boron filaments are presented in figure 8.

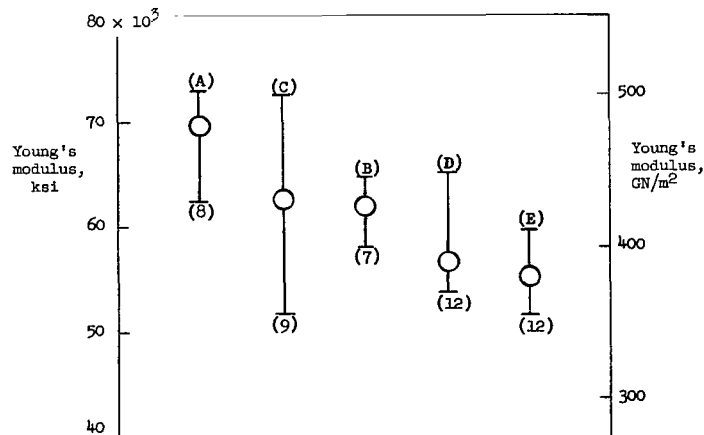


Figure 8.- Average Young's moduli for halide-process boron filaments. Gage length, 10 inches (25.4 cm). Letters in parentheses indicate filament type. Numbers in parentheses indicate number of tests upon which each point is based.

One of the more significant results of the stress-strain study of boron filaments is that no plastic deformation is observed. The stress-strain curve is a straight line. In addition, the scatter in Young's modulus values among specimens of the same filament type is considerably less on a percentage basis than the corresponding scatter in ultimate strength values. Finally, it must be noted that the halide-process boron filaments exhibit a very high stiffness. The average Young's modulus values for the halide-process filaments ranged from  $55 \times 10^3$  to  $70 \times 10^3$  ksi (380 to 480 GN/m<sup>2</sup>), or approximately five times those of the E- and S-glasses currently used in many filament-winding applications. The Young's modulus values of all the organometallic-process boron filaments, which varied from  $18 \times 10^3$  to  $48 \times 10^3$  ksi (110 to 330 GN/m<sup>2</sup>), were lower than those of halide-process filaments. An organometallic-process filament is shown in figure 9. Average Young's modulus curve, moduli and strength values are shown in figure 9. Average Young's modulus values for all the organometallic-process boron filaments tested are presented in figure 10. The low moduli for filaments G and H result from a reduction of the effective filament cross section as a result of polymeric boron hydride inclusions.

#### Elevated-Temperature Tensile Tests

The effect of elevated temperature on the tensile strength of boron filaments A, C, and E is shown in figures 11, 12, and 13.

Figure 11 indicates that the strength remains essentially constant as temperature is increased to approximately 800° F (700° K). At this temperature, a sharp change in the slopes of the curves for tests in both air and argon occurs and strength decreases more rapidly with increasing temperature until at

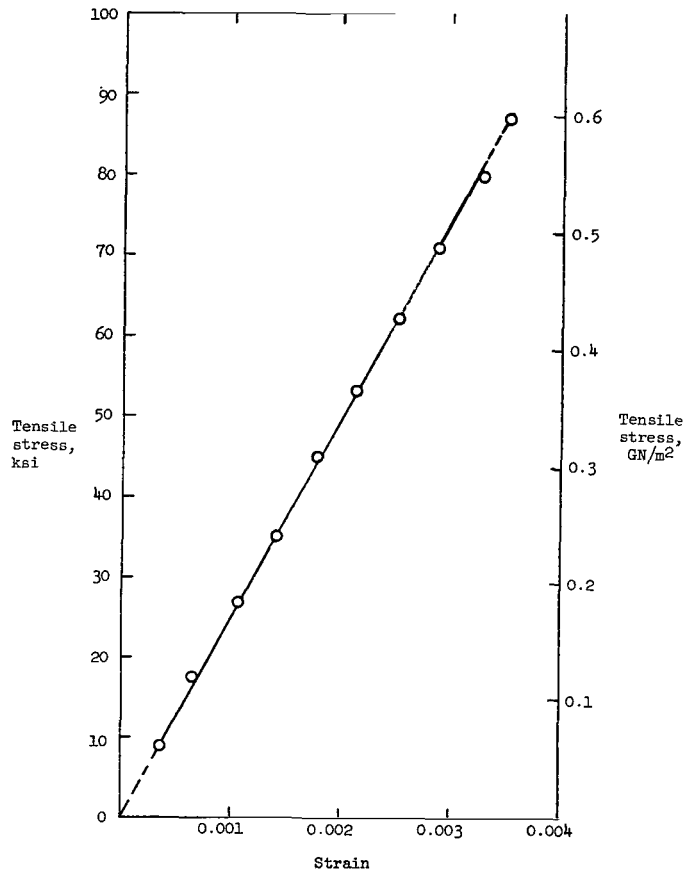


Figure 9.- Typical stress-strain curve for boron filament H. Gage length, 10 inches (25.4 cm). Diameter 0.0038 inch (97  $\mu\text{m}$ ). Dashed segments of curve represent extrapolation of experimental data.

1000° F (811° K) the filament strength is only about half the room temperature value. Another slope change occurs at approximately 1000° F (811° K) after which the strength decrease with increasing temperature becomes more gradual until, at about 1750° F (1227° K), filament strength is for all practical purposes completely diminished. The curve for the filaments tested in air falls below the curve for the filaments tested in argon. It appears that this effect results from surface oxidation that reduces the effective diameter of the filaments in an air atmosphere during testing at elevated temperature.

A differently shaped curve of the variation of strength with temperature is plotted for filament C in figure 12. In this figure, strength slowly decreases with increasing temperature until a temperature of 2000° F (1366° K) is reached. Beyond this temperature, strength decreases very rapidly until at 2250° F (1505° K) it is essentially negligible. Here again, the effect of

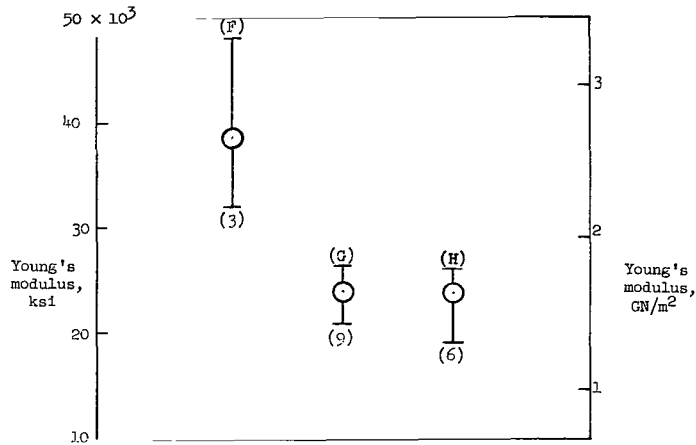


Figure 10.- Average Young's moduli for organometallic-process boron filaments. Gage length, 10 inches (25.4 cm). Letters in parentheses indicate filament type. Numbers in parentheses indicate number of tests upon which each point is based.

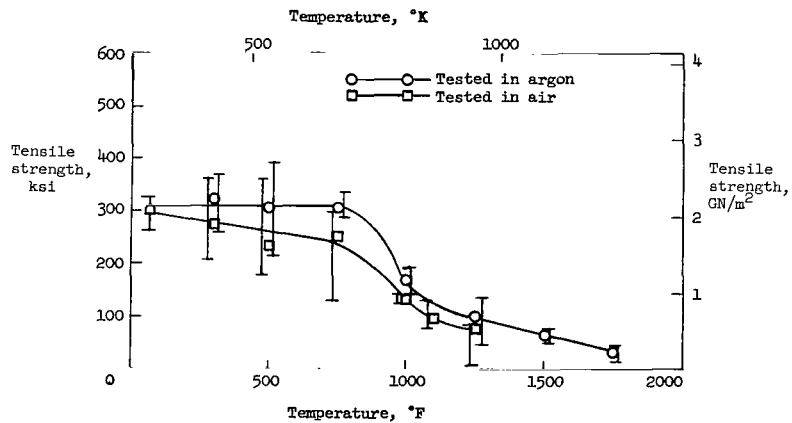


Figure 11.- Effect of temperature on tensile strength of boron filament A. Specimens held at temperature for 60 seconds before load was applied. Each point represents 10 tests. Gage length, 10 inches (25.4 cm).

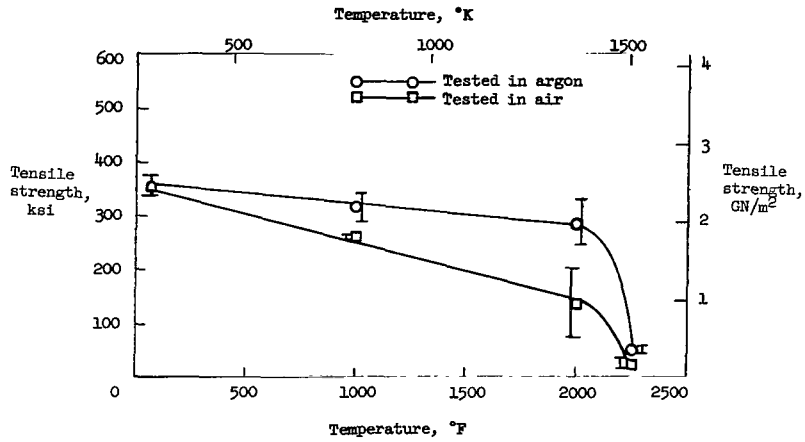


Figure 12.- Effect of temperature on tensile strength of boron filament C. Specimens held at temperature for 60 seconds before load was applied. Each point represents 2 tests. Gage length, 10 inches (25.4 cm).

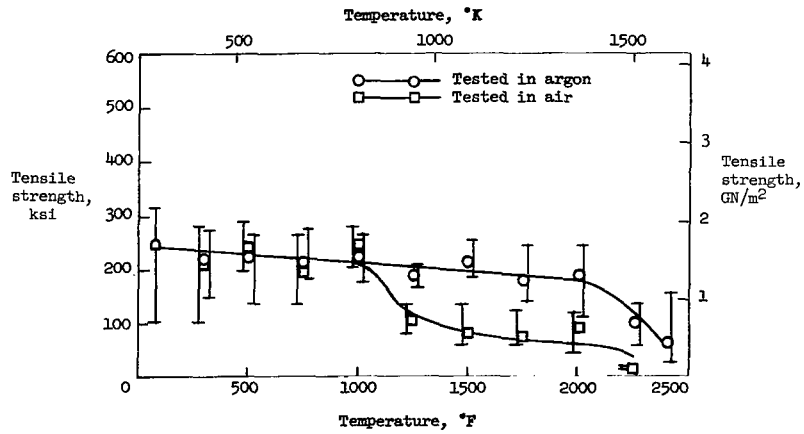


Figure 13.- Effect of temperature on tensile strength of boron filament E. Specimens held at temperature for 60 seconds before load was applied. Each point represents 5 tests. Gage length, 10 inches (25.4 cm).

oxidation is significant not only in reducing strength, but also in increasing the rate at which strength decreases with increasing temperature.

The relation between strength and temperature for filament E is shown in figure 13. The curve for filaments tested in air is similar to both curves determined for filament A (fig. 11) in that it exhibits the double change in slope. It is interesting to note that for filament E (fig. 13) the portions of both curves resulting from tests in air and argon are coincident below 1000° F (811° K) indicating that a protective oxide layer ( $B_2O_3$ ) may possibly have formed (ref. 1). The filaments A, C, and E are identical in composition; the only difference is that filament E was produced from boron tribromide while the other two were produced from  $BCl_3$ . The curves representing tests in argon should provide a more realistic basis for predicting filament strength at elevated temperatures in a practical composite material, if the surface of the filament were shielded from the air by the matrix material.

### Effect of Elevated-Temperature Exposure on Strength

Halide-process boron filaments.- A series of tensile tests were performed at room temperature on filament specimens which had been exposed to elevated temperature for 15 minutes in still air and in a vacuum of  $1 \times 10^{-5}$  torr ( $1.33 \text{ mN/m}^2$ ). Figures 14 and 15 show the results of these tests of filaments A and C. Each test point represents the average of 10 tests. It can be seen that elevated-temperature exposure in vacuum reduces the strength of the filaments only slightly. The effect was more severe when the specimens were exposed in air because of oxidation of the filament surfaces.

Organometallic-process boron filaments.- After exposure to elevated temperature in a vacuum, organometallic-process filaments were found to be almost

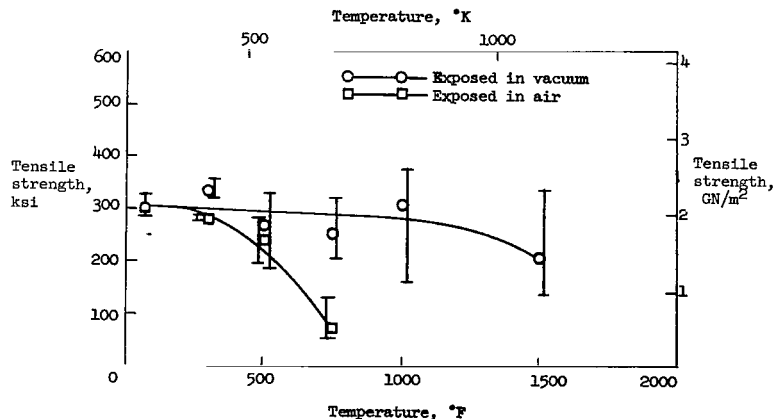


Figure 14.- Effect of elevated-temperature exposure on tensile strength of boron filament A. Exposure time, 15 minutes. Gage length, 10 inches (25.4 cm). Each point represents 10 tests.

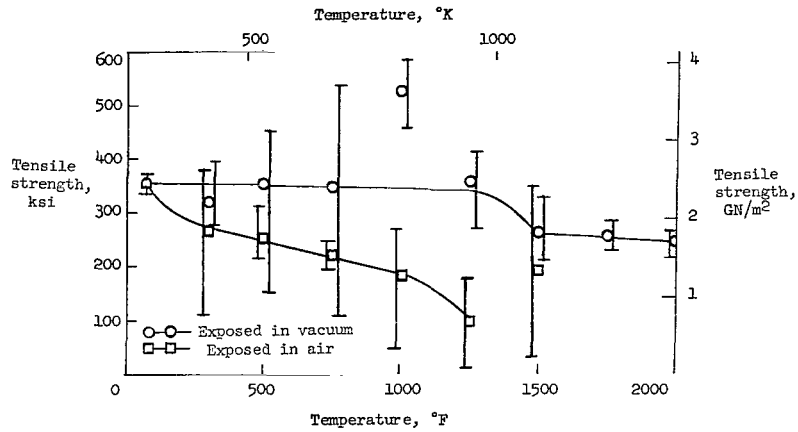
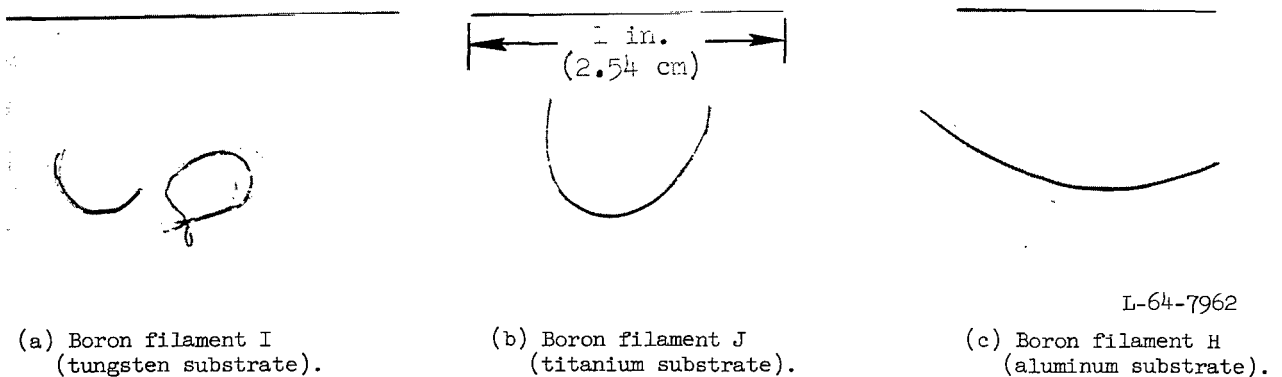


Figure 15.- Effect of elevated-temperature exposure on tensile strength of boron filament C. Exposure time, 15 minutes. Gage length, 10 inches (25.4 cm). Each point represents 5 tests.

completely destroyed (fig. 16). The straight specimens shown in the figure were exposed 30 minutes at 750° F (672° K). The curved specimens were exposed for 30 minutes at 1000° F (811° K). The higher exposure temperature in this case was sufficient to cause the metallic substrate wire to react with the boron sheath to form metal borides. The thermal contraction differential between the boride core and the surrounding boron was sufficient to cause the filaments to kink and curl upon cooling from the exposure temperature to room temperature. The stresses developed in this manner caused many small cracks to form in the filament specimens and thereby reduced the strength to essentially zero. This effect was observed only in organometallic-process filaments which were produced at temperatures below 1000° F (811° K). If the reaction between the boron and metal substrate occurs during production of the filament while the substrate wire is at high temperature and under tension, the resulting filament is straight at room temperature and has appreciable strength. This is



L-64-7962

- (a) Boron filament I (tungsten substrate). (b) Boron filament J (titanium substrate). (c) Boron filament H (aluminum substrate).

Figure 16.- Effect of elevated-temperature exposure on physical appearance of filaments made from diborane. Straight specimens exposed 30 minutes at 750° F (672° K), and  $1 \times 10^{-5}$  torr ( $1.3 \text{ mN/m}^2$ ) pressure; curved specimens exposed 30 minutes at 1000° F (811° K), and  $1 \times 10^{-5}$  torr ( $1.3 \text{ mN/m}^2$ ) pressure.

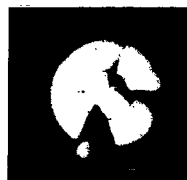
the case with all the halide-process filaments and the higher temperature organometallic-process filaments. However, these filaments are residually stressed because of the thermal contraction differential between the boron and the boride core. The effect of this residual stress on mechanical properties is probably detrimental.

### Metallographic Examination

Hardness measurements.- The relative hardnesses of the boride core, boron sheath, and core-boron interface are illustrated in figure 17 by a series of photomicrographs of the same boron filament C cross section at various stages of a diamond polishing operation. In figure 17(a), the cross section is shown after rough grinding on 600 grit paper. In figure 17(b), the cross section is shown after 8 hours in diamond paste on a vibrating cloth-covered platform. The specimen has been considerably flattened, and the outline of the core-boron interface can be seen. The dark wedge in the lower portion of the boron sheath is a segment which is raised in relief, and is out of focus at this magnification. Figures 17(c) and 17(d) show the progressive delineation of the center of the boride core and the core-boron interface relative to the remainder



(a) Cross section after grinding on 600 grit paper.



(b) Cross section after 8 hours in diamond paste.



(c) Cross section after 16 hours in diamond paste.



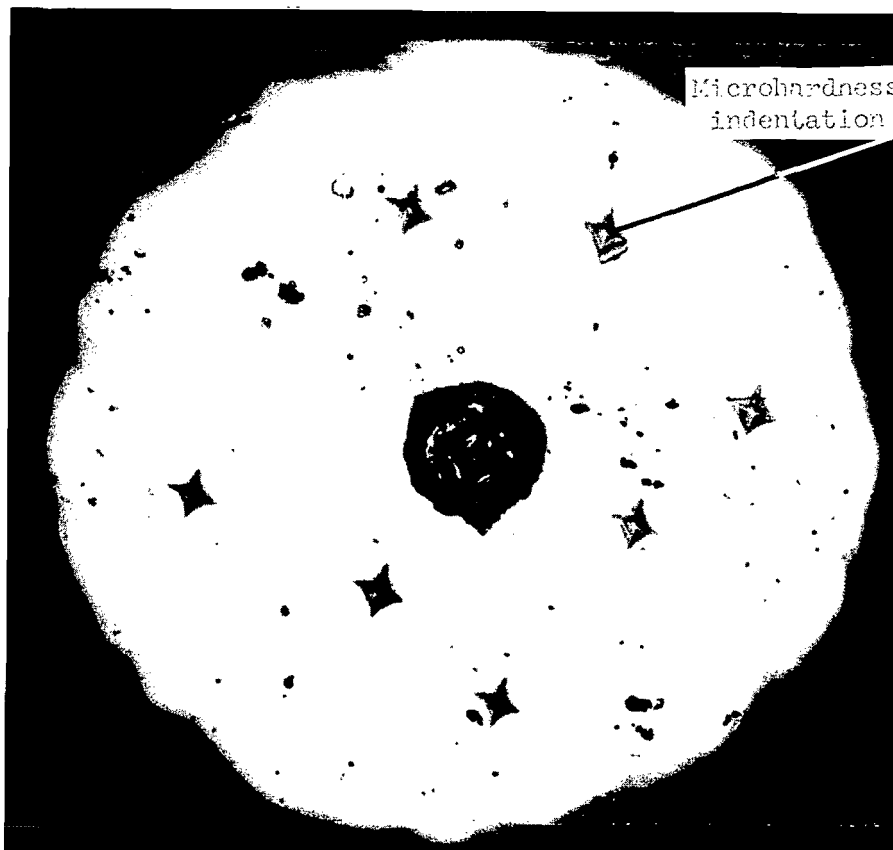
(d) Cross section after 32 hours in diamond paste.

L-65-7935

Figure 17.- Photomicrographs of typical halide-process boron filament cross section at various degrees of polish; illustrating the relative hardnesses of the core, boron sheath, and core-sheath interface. Filament diameter, 0.0046 inch (0.117 mm). Polishing accomplished on a vibrating cloth impregnated with 6-micron (6- $\mu$ m) diamond paste.

of the filament. The center of the core contains borides that are richest in tungsten and, therefore, should be the softest area of the filament section. The interface, however, because it is highly stressed, should be very hard brittle. The material at the interface was probably removed by fragmentation due to brittleness rather than by wear caused by abrasion.

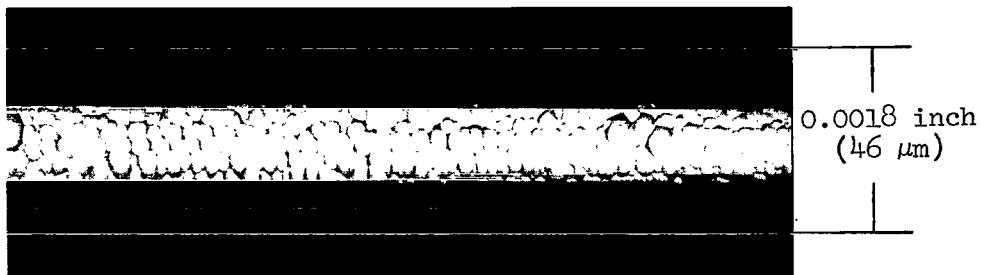
Microhardness measurements were made on similar filament C cross sections using a  $136^\circ$  (2.38 rad) diamond pyramid indenter under a 0.1 kgf (0.98 N) load. A photomicrograph of a typical cross section showing the DPH (diamond pyramid hardness) indentations is shown in figure 18. The cracks emanating from the core resulted from the last indentation which was placed directly in the center of the core. Although hardness measurements were made at various distances from the filament center, no hardness variation with radial distance was observed. The average hardness of the boron sheath was determined to be 3755 DPH, and the average hardness of the core was 2371 DPH. The data from all the hardness measurements are presented in table III. The hardness values are very high as would be expected when the high modulus and strength of the filaments are considered. There is no direct correlation between DPH numbers and Knoop hardness values. However, the relative position of the values observed



L-65-7936  
Figure 18.- Photomicrograph of polished cross section of boron filament C showing microhardness indentations. Diameter, 0.0046 inch (0.117 mm). Indentations made with a 0.1-kgf (0.98-N) load on a  $136^\circ$  (2.38-rad) diamond pyramid.

in this study on the DPH scale as compared with the Knoop scale, indicates that the hardness of the boron filaments studied is roughly equivalent to that of silicon carbide based on values published in reference 1.

Boron-filament surfaces.- The surface of a typical halide-process boron filament (fig. 19) has a rough, pebbly appearance somewhat resembling an ear of corn. Although more pronounced in the case of boron filaments, this type



L-65-7937

Figure 19.- Typical halide-reduction-process filament surface; diameter, 0.0018 inch (46 μm).

of surface is often found on vapor-deposited materials, for example, pyrolytic graphite. Photomicrographs of organometallic-process filaments H, J, I, and L; and samples of their respective substrates are shown in figures 20 to 23, respectively. Filament H (fig. 20(a)) was produced by the vapor deposition of boron onto aluminum wire (fig. 20(b)). The aluminum wire, being soft and not subject to severe die marking during drawing, has a relatively smooth surface and the resultant filament has a smooth surface. Filament J (fig. 21(a)) has a rough surface. It was produced on titanium substrate wire (fig. 21(b)) which is difficult to draw, and has a correspondingly rough surface. Filaments I and L (figs. 22(a) and 23(a)) were produced on tungsten wire (figs. 22(b) and 23(b)) which also has a rough surface. This wire is similar to that used to make the halide-process filaments. The surface of filaments I and L, however, is much smoother and indicates that the surface characteristics of a boron filament do not depend only on the condition of the substrate surface. It has generally been assumed that the pebbly surface was a result of the reproduction of substrate surface imperfections (die markings) by the vapor-deposition process. Actually, the roughness of the filament surface is probably determined to a large extent by the control of interrelating variables of the vapor-deposition process.

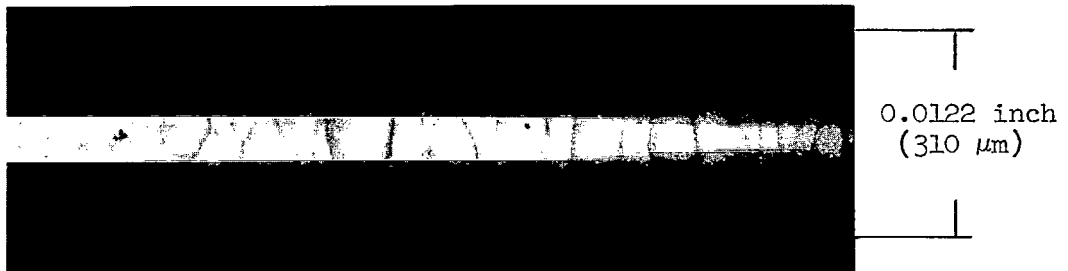


(a) Boron filament; diameter, 0.0126 inch (320  $\mu\text{m}$ ).



L-65-7938  
(b) Aluminum substrate wire; diameter, 0.001 inch (25  $\mu\text{m}$ ).

Figure 20.- Surfaces of boron filament H and substrate wire.

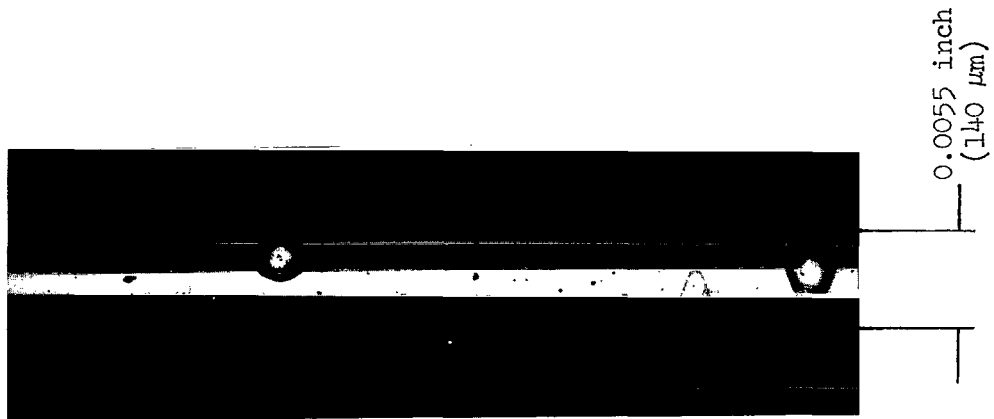


(a) Boron filament; diameter, 0.0122 inch (310  $\mu\text{m}$ ).

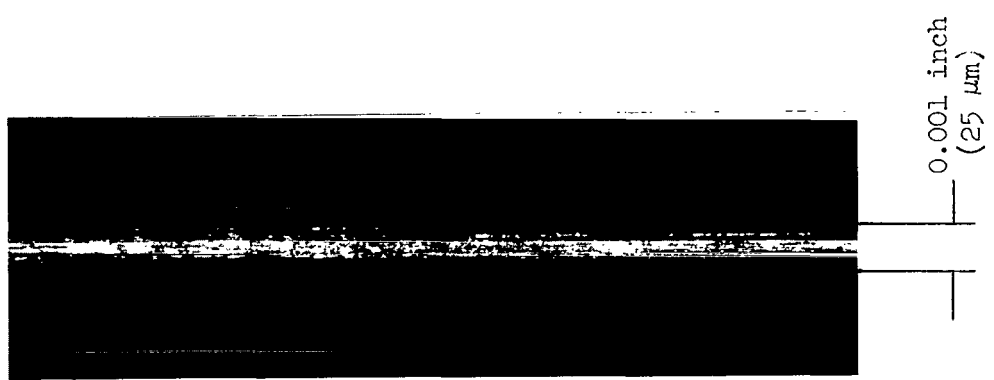


(b) Titanium substrate wire; diameter, 0.001 inch (25  $\mu\text{m}$ ).  
L-65-7939

Figure 21.- Surfaces of boron filament J and substrate wire.



(a) Boron filament; diameter, 0.0055 inch (140 μm).



(b) Tungsten substrate wire; diameter, 0.001 inch (25 μm).  
L-65-7940

Figure 22.- Surfaces of boron filament I and substrate wire.



(a) Boron filament; diameter, 0.0051 inch (130  $\mu\text{m}$ ).



L-65-7941  
(b) Tungsten substrate wire; diameter, 0.001 inch (25  $\mu\text{m}$ ).

Figure 23.- Surfaces of boron filament L and substrate wire.

Boron-filament sections.- Photomicrographs of several cross sections of a typical halide-process boron filament are presented in figure 24. A few cracks were observed after the sections were cut, and the number increased noticeably during grinding and polishing. The cracks appear to substantiate the presence of residual stresses which exist between the boride core and the boron sheath as a result of the thermal contraction differential which occurs as the filament cools from the deposition temperature. The abrasive particles rolling and sliding over the section surface apparently cause the initiation and propagation of additional cracks.



L-65-7942  
Figure 24.- Photomicrograph showing typical polished cross sections of halide-process boron filament. Diameter, 0.0046 inch (0.117 mm).

Two cross sections of organometallic process filament H are presented in figure 25. These filaments were produced at a temperature low enough so that the boride-forming reaction did not take place in the core. The cores shown in these photomicrographs are composed of metallic aluminum. The diagonal lines which are visible on the section surfaces are scratches resulting from grinding. The dark areas which resemble inclusions are areas where boron has been removed in the form of small chips by the action of the abrasive grit. The cross section on the left was cut from a filament which had been produced on substrate wire with an oval cross section. The elliptical shape of the substrate is reproduced by the vapor deposition process. This result suggests that a variety of shapes more suitable for filament winding might be produced if properly shaped substrate wire were available.

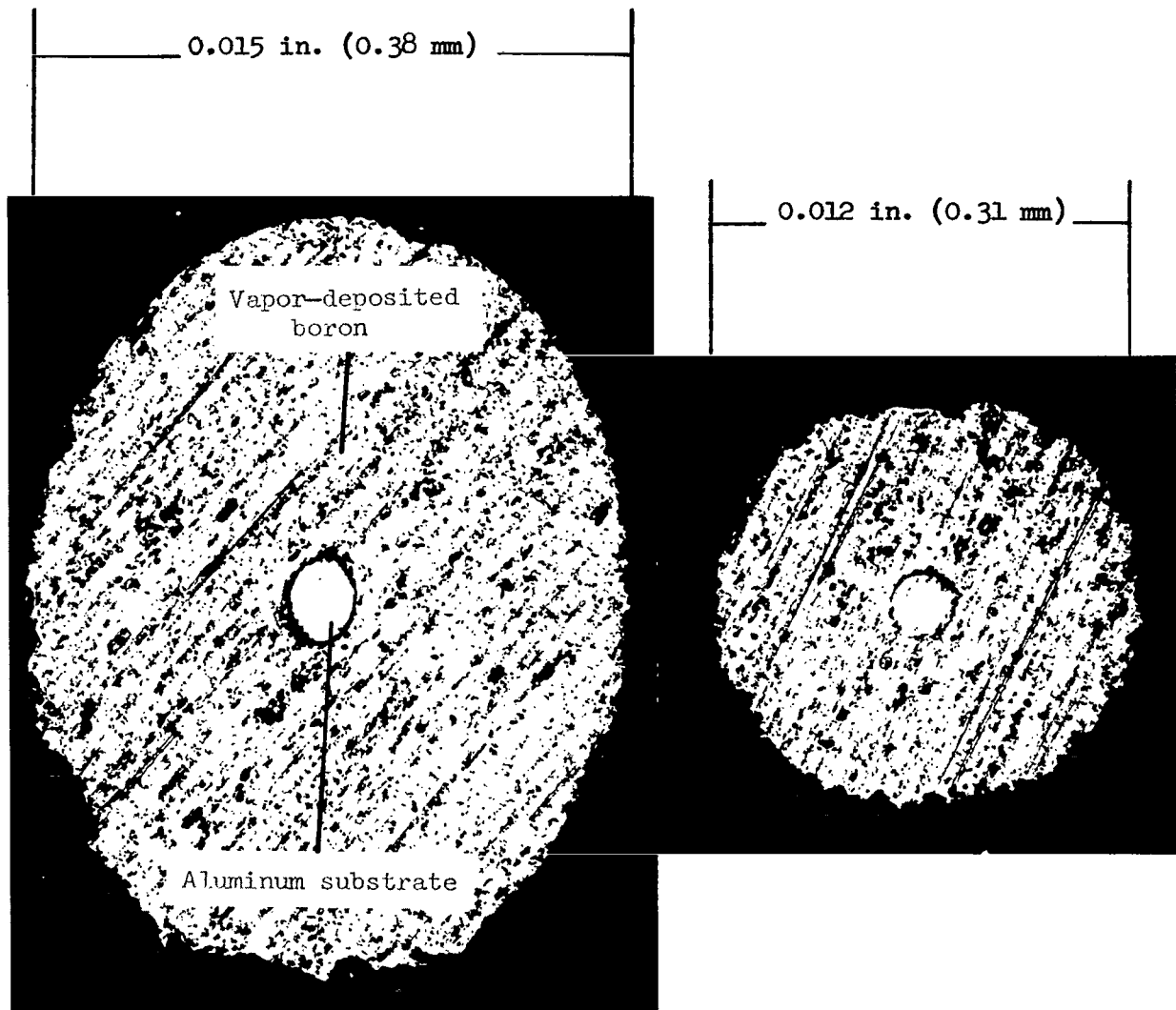


Figure 25.- Cross sections of boron filament H made from diborane on aluminum substrate wire. L-65-7943

Fracture modes.- Typical boron filament fracture surfaces after tensile failure are shown in figure 26 for filament F. The annular rings near the substrate core, however, were observed only in the case of a few organometallic-process filaments. Although filament failure was very rapid at the ultimate stress in tension, it appears that the mechanism of fracture involved the formation and propagation of cracks in such a manner that a small wedge of boron was usually split out of the side of the filament. This result can be seen in

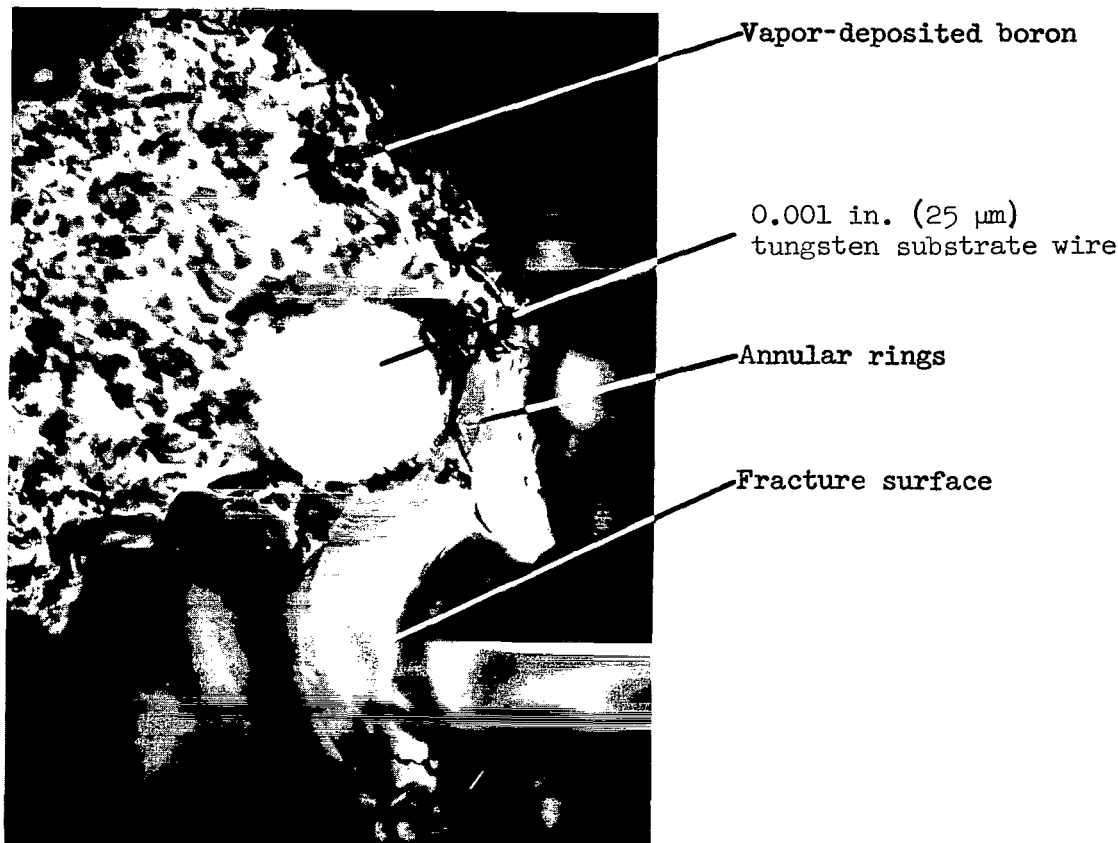
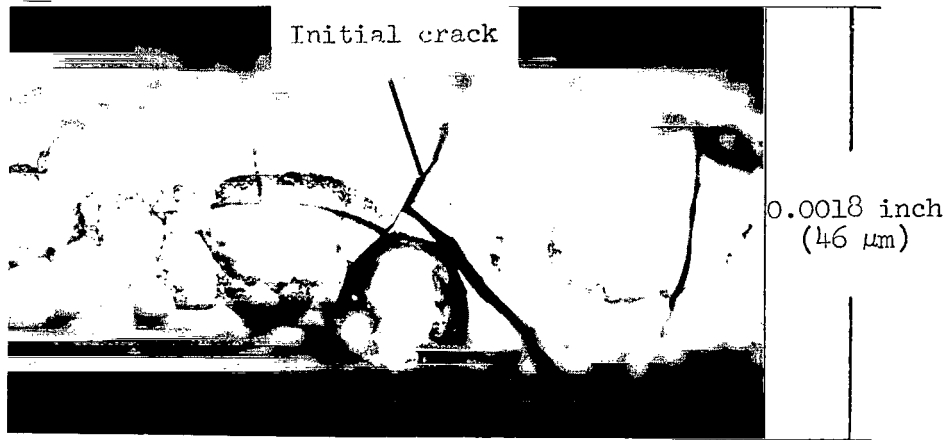
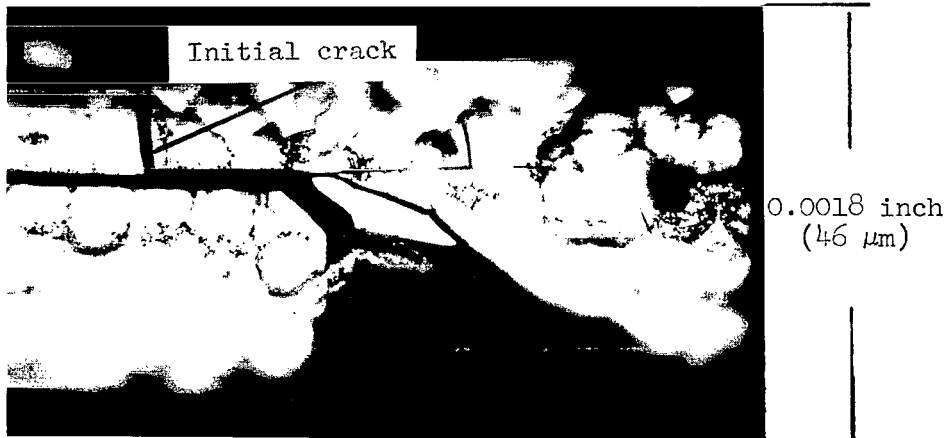


Figure 26.- Photomicrograph of boron filament F cross section showing fracture surfaces. L-65-7944  
X1000.

the case of tensile failure of two separate halide-process-filament specimens shown in figure 27. These fractures were artificially initiated by choosing low-strength specimens which contained one existing circumferential crack and taking photomicrographs of the areas containing the cracks after the specimens had been subjected to a slight tensile stress. In figure 27(a), the initial crack has propagated to such extent that the shape of the wedge is outlined although it has not yet separated from the filament. In figure 27(b), a different specimen has undergone complete fracture, and a small wedge of boron is seen to have separated completely from the filament.



(a)



(b)

L-65-7945  
Figure 27.- Typical appearance of halide-process boron filaments at instant of tensile fracture. Diameter, 0.0018 inch (46  $\mu\text{m}$ ).

## CONCLUDING REMARKS

A study was made to determine selected mechanical and physical properties of 12 types of boron filaments. The results of the study are as follows:

1. Boron filaments made by a boron-halide-reduction process exhibit high strength and elastic modulus. The results of room-temperature tensile tests indicate that on the average these boron filaments possess strength (350 ksi (2.42 GN/m<sup>2</sup>)) which is comparable with that of commercially available glass filaments, and elastic modulus ( $60 \times 10^3$  ksi (414 GN/m<sup>2</sup>)) which is five times as great as that of glass filaments.
2. The halide-process filaments have a hardness of 3755 DPH (diamond pyramid hardness), which is about the same as that for silicon carbide.
3. Boron filaments made by vapor deposition from organometallic compounds exhibit low strength and elastic modulus relative to values for halide-process filaments.
4. Because of the brittle nature of the filaments, considerable scatter is obtained in the values of tensile strength. The scatter in elastic modulus is much less on a percentage basis than the scatter in tensile strength.
5. The tensile strengths of halide-process boron filaments are found to be only slightly reduced at temperatures up to 2000° F (1366° K) in an inert atmosphere. When similar tests are conducted in atmospheric air, filament tensile strength is significantly reduced.

Langley Research Center,  
National Aeronautics and Space Administration,  
Langley Station, Hampton, Va., September 17, 1965.

APPENDIX A

CONVERSION OF U.S. CUSTOMARY UNITS TO SI UNITS

The International System of Units (SI) was adopted by the Eleventh General Conference on Weights and Measures, Paris, October 1960, in Resolution No. 12 (ref. 4). Conversion factors for the units used herein are given in the following table:

Physical quantity	U.S. Customary Unit	Conversion factor (*)	SI Unit
Angle . . . . .	deg	$1.745329 \times 10^{-2}$	radians (rad)
Flow rate . . . . .	ft <sup>3</sup> /hr	7.8656	cu. centimeters/second (cm <sup>3</sup> /s)
Length . . . . .	in.	0.0254	meters (m)
Load . . . . .	lbf	4.448222	newtons (N)
Mass . . . . .	lbm	454	grams (g)
Pressure . . . . .	torr	133.322	newtons per sq meter (N/m <sup>2</sup> )
Stress . . . . .	ksi = 1000 lbf/in <sup>2</sup>	$6.895 \times 10^6$	newtons per sq meter (N/m <sup>2</sup> )
Temperature . . . . .	°F	$(5/9)(°F + 459.67)$	degrees Kelvin (°K)
			1 kgf × 9.80665 = 1 newton (N)

\*Multiply value given in U.S. Customary Unit by a conversion factor to obtain equivalent value in SI Units.

Prefixes to indicate multiple of units are as follows:

Prefix	Multiple
micro (μ)	10 <sup>-6</sup>
milli (m)	10 <sup>-3</sup>
centi (c)	10 <sup>-2</sup>
kilo (k)	10 <sup>3</sup>
giga (G)	10 <sup>9</sup>

## APPENDIX B

### STATISTICAL ANALYSIS OF SELECTED TENSILE DATA

In an effort to examine the problem of scatter in the determination of filament mechanical properties more closely, a tensile failure stress histogram (fig. 28) was plotted for the previously selected 120 test population of filaments. An attempt was made to determine the reliability of the experimentally

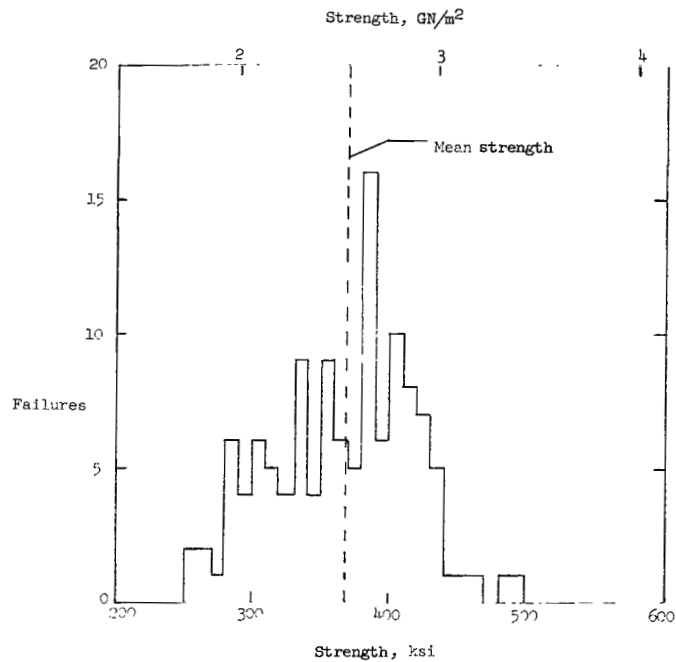


Figure 28.- Frequency histogram of tensile failures for boron filament A, reel 1. Frequency based on 1-inch (2.54-cm) gage length, 10 ksi (0.069 GN/m<sup>2</sup>) stress intervals, and 120 tests.

determined relationship between strength and gage length of filament A (fig. 6) based on a statistical analysis of the distribution of tensile failures of 1-inch (2.54-cm) gage length specimens (table II). The distribution was plotted (fig. 29) on normal probability coordinates and was found to approximate the normal distribution closely. The distribution curve was based on 120 tensile tests grouped in 5-ksi (0.035-GN/m<sup>2</sup>) stress intervals.

Weibull (ref. 9) proposed an empirical distribution function which has been found to describe the distribution of brittle-material tensile failures quite well. For the purpose of this investigation, Weibull's function may be written as

APPENDIX B

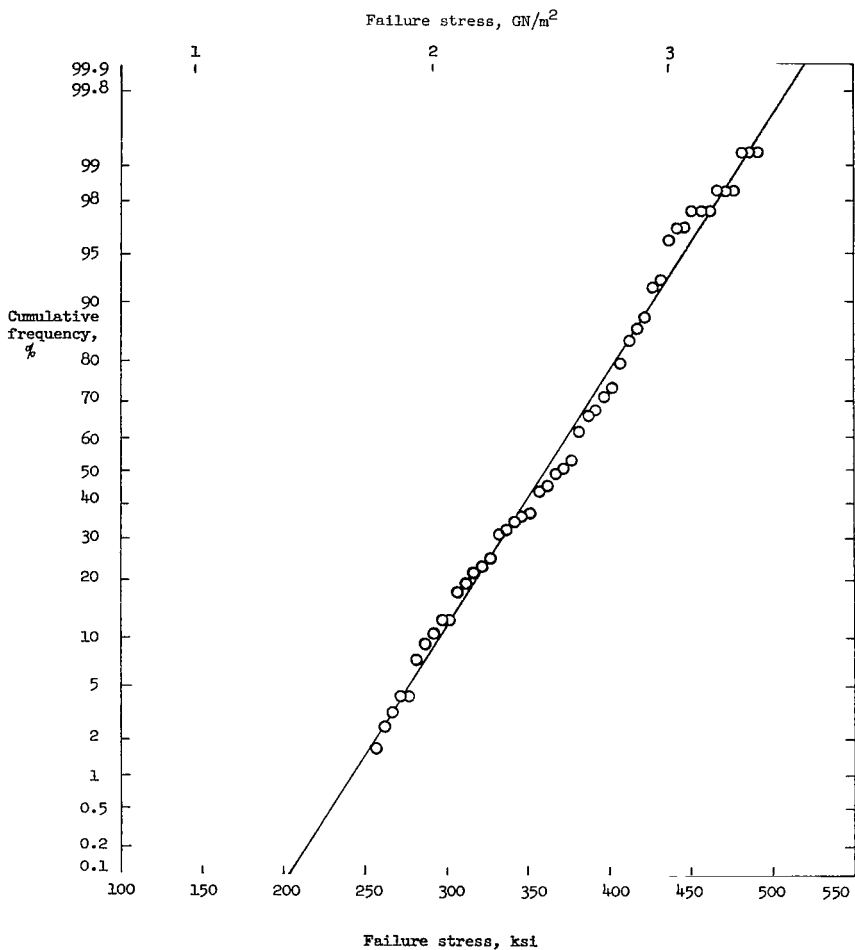


Figure 29.- Cumulative failure frequency plot on normal probability scale for boron filament A, reel no. 1. Gage length, 1 inch (2.54 cm).

APPENDIX B

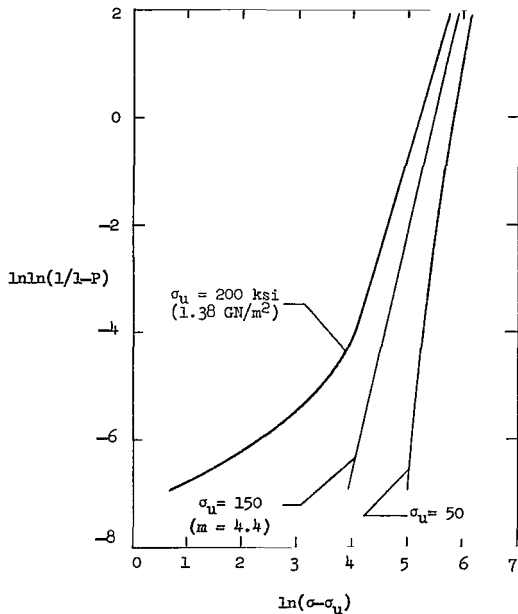


Figure 30.- Plot of Weibull's distribution function parameters for 120 tensile failures of boron filament A, reel 1. Gage length, 1 inch (2.54 cm).

$$P = 1 - e^{-L \left( \frac{\sigma - \sigma_u}{\sigma_o} \right)^m} \quad (1)$$

where

- P probability of specimen failure
- e base of Napierian logarithm
- L filament gage length (the form of the inclusion of L in eq. (1) is suggested in ref. 10)
- $\sigma$  filament failure stress
- $\sigma_u$  lower bound of distribution (value of  $\sigma$  for which  $P = 0$ )
- m distribution shape factor
- $\sigma_o$  distribution scale factor

Rearranging the Weibull function, and taking the logarithm of both sides twice gives

$$\ln \ln(1/1 - P) = m \left[ \ln(\sigma - \sigma_u) - \ln \sigma_o \right] + \ln L \quad (2)$$

Corresponding values of P and  $\sigma$  were determined directly from the normal distribution plot (fig. 29). Using these values, and values of  $\sigma_u$  assumed at random, the quantities  $\ln \ln(1/1 - P)$  and  $\ln(\sigma - \sigma_u)$  were calculated and plotted in figure 30. From equation (2) it is seen that the correctly assumed value of  $\sigma_u$  will result in a straight-line plot of  $\ln \ln(1/1 - P)$  against  $\ln(\sigma - \sigma_u)$ . The shape factor, m, is the slope of the straight line thus obtained. For the distribution of filament A specimens, the lower bound was determined to be  $\sigma_u = 150$  ksi (1.04GN/m<sup>2</sup>) and the shape factor,  $m = 4.4$ . By substituting these values into equation (2), the scale factor is determined to be  $\sigma_o = 236$  ksi (1.63 GN/m<sup>2</sup>). Equation (1) was then solved for varying gage lengths up to 500 inches (12.7 m) at probability levels of 1, 50, and 99 percent. The results are shown as dashed curves (fig. 31) superimposed over the data points from the plot of strength against gage length for filament A (fig. 6).

## APPENDIX B

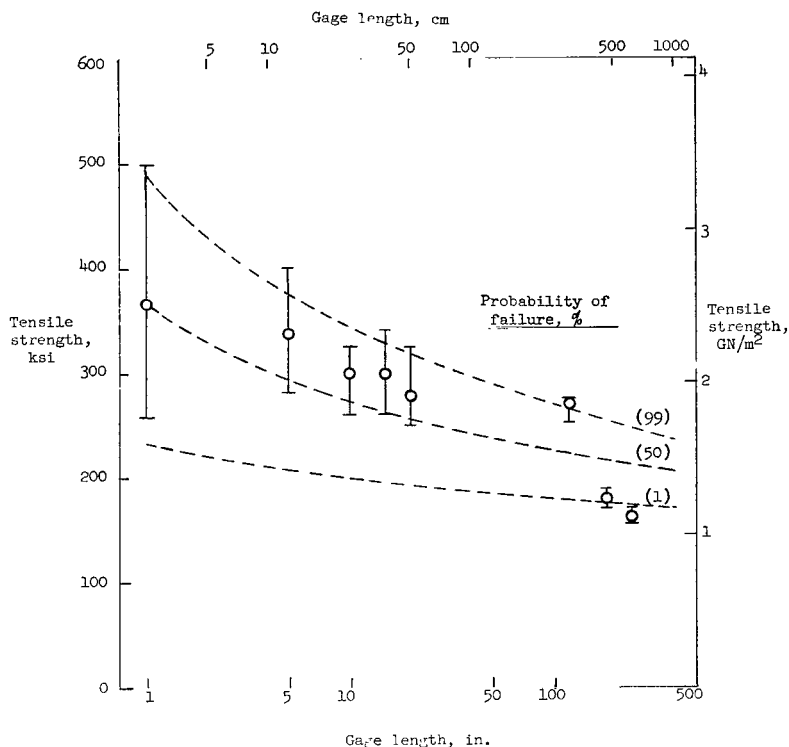


Figure 31.- Tensile strength of boron filament A, reel 1 as a function of gage length. Dashed lines represent constant-probability curves generated from an analysis of the distribution of 120 test breaks of 1-inch (2.54-cm) gage-length specimens based on the Weibull distribution function.

The 50-percent-probability curve represents the probability that half of the specimens tested will fall above, and half below the curve. The accurate location of this curve, however, depends on whether the distribution of the 120 test samples of 1-inch (2.54-cm) gage length specimens is an accurate representation of the entire population of boron filaments of this type. It is possible that the sample was not representative and that more tests would be required before the isoprobability curves could be located with a higher degree of certainty.

The calculated probability curves do not agree very well with the experimental data. Specimens with gage lengths of 5, 10, 15, 20, and 120 inches (12.7, 25.4, 38.1, 50.8, and 305 cm) exhibit an average failure stress well above the 50-percent-probability curve. Several of the specimens from these groups survived at a stress level at which 99 percent of all specimens should fail. Specimens with gage lengths of 180 and 240 inches (457 and 610 cm), however, exhibit average strengths considerably below the 50-percent curve. A few failed at a stress at which 99 percent of all specimens should survive.

## APPENDIX B

The lack of agreement between the calculated probability curves and the experimentally obtained data is not unexpected. The accuracy of the statistical analysis depends on the validity of two hypotheses: One, that Weibull's function describes the distribution of boron-filament tensile strengths; and two, that the 120 test population upon which the analysis is based is a true statistical sample. The lack of agreement may be partly due to a failure of the Weibull function to apply in the case of boron-filament tensile failure. However, the major portion of the difficulty is believed to result from the fact that the 120 test sample used is not truly statistical.

The data from the 120 tensile tests of 1-inch (2.54-cm) gage-length specimens are listed in the first portion of table III consecutively, as they were taken off the reel. If these data are plotted (fig. 32) as a function of distance from the end of the reel, a decrease in filament strength is observed as

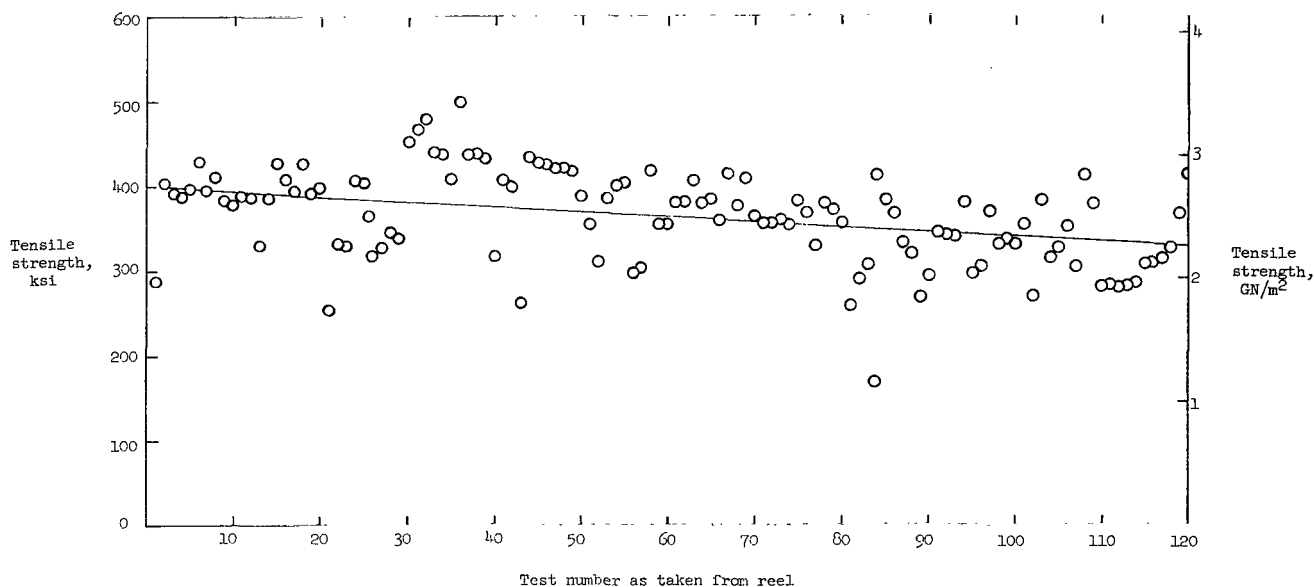


Figure 32.- Tensile strength of boron filament A. Reel 1; 120 tests of 1-inch (2.54-cm) gage-length specimens plotted consecutively as removed from the reel.

the number of specimens removed from the reel is increased. This decrease is apparently due to the process by which the filaments were manufactured. This trend, which is exhibited in figure 32, probably accounts for a large portion of the lack of agreement between the calculated and experimental curves, since it is not taken into account by the statistical analysis. The analysis is based on the assumption that the 120 tensile strengths of 1-inch (2.54-cm) gage-length specimens do not exhibit a trend of any kind but are randomly distributed - not artificially randomized by the plotting of a distribution curve (fig. 29).

## REFERENCES

1. Kohn, J. A.; Nye, W. F.; and Gaule, G. K., eds.: Boron - Synthesis, Structure, and Properties. Plenum Press, Inc., 1960.
2. Witucki, Robert M.: Boron Filaments. ARC-R-107, Astro Res. Corp., Sept. 12, 1963.
3. Witucki, Robert M.: Boron Filaments. NASA CR-96, 1964.
4. Mechtly, E. A.: The International System of Units - Physical Constants and Conversion Factors. NASA SP-7012, 1964.
5. Laubengayer, A. W.; Hurd, D. T.; Newkirk, A. E.; and Hoard, J. L.: Boron. I. Preparation and Properties of Pure Crystalline Boron. J. Am. Chem. Soc., vol. 65, 1943, pp. 1924-1931.
6. Newkirk, Arthur E.: Preparation and Chemistry of Elementary Boron. Advances in Chemistry Series, No. 32, Robert F. Gould, ed., Am. Chem. Soc., 1961, pp. 27-41.
7. Powell, C. F.; Campbell, I. E.; and Gonser, B. W.: Vapor-Plating. John Wiley & Sons, Inc., 1955.
8. Rosen, Walter B.: Tensile Failure of Fibrous Composites. AIAA J., vol. 2, no. 11, Nov., 1964, pp. 1985-1991.
9. Weibull, Waloddi: A Statistical Distribution Function of Wide Applicability. J. Appl. Mech., vol. 18, no. 3, Sept. 1951, pp. 293-297.
10. Metcalfe, A. G.; and Schmitz, G. K.: Effect of Length on the Strength of Glass Fibers. Preprint No. 87, Am. Soc. for Testing Mater., 1964.

TABLE I.- SUMMARY OF FILAMENT TYPES INVESTIGATED

Filament	Type	Substrate	Starting compound	Manufacturer
A	Boron	Tungsten	$\text{BCl}_3 + \text{H}_2$	United Aircraft Corp. East Hartford, Conn.
B	Boron	Tungsten	$\text{BCl}_3 + \text{H}_2$	} Texaco Experiment, Inc. Richmond, Va.
C	Boron	Tungsten	$\text{BCl}_3 + \text{H}_2$	
D	Boron	Tungsten	$\text{BCl}_3 + \text{H}_2$	General Electric Co. Flight Propulsion Div. Cincinnati, Ohio
E	Boron	Tungsten	$\text{BBr}_3 + \text{H}_2$	Astro Research Corp. Santa Barbara, Calif.
F	Boron	Tungsten	$\text{B}_2\text{H}_6$	} General Technologies Corp. Alexandria, Va.
G	Boron	Aluminum	$\text{B}_5\text{H}_9$	
H	Boron	Aluminum	$\text{B}_2\text{H}_6$	
I	Boron	Tungsten	$\text{B}_2\text{H}_6$	
J	Boron	Titanium	$\text{B}_2\text{H}_6$	
K	Boron	Tungsten	$\text{B}_5\text{H}_9$	
L	Boron	Tungsten	$(\text{C}_2\text{H}_5)_3\text{B}$	

TABLE II.- DATA ON ROOM-TEMPERATURE TENSILE STRENGTH

[Specimens are listed in order they were removed from reel]

Gage length		Ultimate stress	
in.	cm	ksi	GN/m <sup>2</sup>
Filament A from reel 1; average strength, 366 ksi (2.53 GN/m <sup>2</sup> )			
1	2.54	288	1.99
		404	2.79
		391	2.70
		387	2.67
		397	2.74
		429	2.96
		395	2.72
		410	2.85
		382	2.64
		377	2.60
		388	2.68
		387	2.68
		330	2.28
		386	2.66
		427	2.95
		408	2.82
		395	2.72
		428	2.96
		393	2.71
		399	2.75
		255	1.76
		333	2.30
		330	2.82
		407	2.81
		405	2.80
		318	2.19
		329	2.27
		348	2.39
		339	2.34
		453	3.13
		468	3.23
		480	3.31
		440	3.04
		438	3.02
		409	2.82
		499	3.44
		457	3.02
		438	3.02
		433	2.99
		318	2.19

Gage length		Ultimate stress	
in.	cm	ksi	GN/m <sup>2</sup>
Filament A from reel 1; average strength, 366 ksi (2.53 GN/m <sup>2</sup> )			
1	2.54	406	2.80
		400	3.76
		263	1.81
		435	3.00
		428	2.96
		426	2.94
		421	2.90
		421	2.90
		417	2.88
		389	2.68
		355	2.45
		311	2.14
		385	2.66
		401	2.77
		405	2.80
		299	2.06
		305	2.10
		419	2.89
		355	2.45
		356	2.46
		382	2.64
		382	2.64
		407	2.81
		380	2.63
		384	2.65
		360	2.48
		415	2.86
		377	2.60
		410	2.83
		365	2.52
		357	2.46
		357	2.46
		361	2.49
		355	2.45
		383	2.64
		369	2.54
		330	2.28
		380	2.62
		372	2.59
		356	2.46

Gage length		Ultimate stress	
in.	cm	ksi	GN/m <sup>2</sup>
Filament A from reel 1; average strength, 366 ksi (2.53 GN/m <sup>2</sup> )			
1	2.54	259	1.79
		290	2.00
		307	2.12
		413	2.85
		383	2.64
		368	2.54
		334	2.30
		320	2.20
		268	1.85
		294	2.03
		345	2.38
		343	2.36
		340	2.34
		381	2.63
		296	2.04
		306	2.11
		370	2.55
		331	2.28
		337	2.32
		331	2.28
		355	2.45
		270	1.86
		383	2.64
		315	2.18
		326	2.25
		351	2.42
		305	2.10
		413	2.85
		379	2.62
		281	1.94
		284	1.89
		280	1.93
		281	1.94
		285	1.97
		306	2.11
		309	2.13
		314	2.16
		326	2.25
		366	2.52
		414	2.86

TABLE II.- DATA ON ROOM-TEMPERATURE TENSILE STRENGTH - Continued

[Specimens are listed in order they were removed from reel]

Gage length		Ultimate stress		Gage length		Ultimate stress					
in.	cm	ksi	GN/m <sup>2</sup>	in.	cm	ksi	GN/m <sup>2</sup>				
Filament A from reel 1				Filament A from reel 1							
5	12.7	402	2.78	15	38.1	285	1.97				
		317	2.19			282	1.95				
		303	2.09			268	1.85				
		368	2.54			296	2.04				
		282	1.95			337	2.32				
		374	2.58			269	1.86				
		324	2.24			306	2.11				
		342	2.36			303	2.09				
		352	2.43			313	2.16				
		324	2.24			282	1.95				
						397	2.74			322	2.22
						353	2.44			301	2.08
						295	2.04			287	1.98
						371	2.56			294	2.03
						309	2.13			301	2.08
						345	2.38	Average strength			
						360	2.48	20	50.8	296	2.04
		329	2.27	250	1.72						
		321	2.22	260	1.79						
		311	2.15	295	2.04						
Average strength		339	2.34	323	2.23						
				257	1.77						
10	25.4	327	2.26	250	1.73						
		310	2.14	271	1.87						
		327	2.26	278	1.92						
		287	1.98	327	2.26						
		313	2.16								
		264	1.82	282	1.95						
		282	1.95	264	1.82						
		306	2.11	308	2.12						
		303	2.09	311	2.15						
		292	2.02	255	1.76						
				279	1.93						
				288	1.99						
				292	2.02						
				259	1.79						
				268	1.85						
				311	2.15						
				266	1.84						
		299	2.06								
		288	1.99								
		315	2.18								
		315	2.18								
		306	2.11								
Average strength		301	2.08	Average strength		281	1.94				
15	38.1	289	1.99	120	305	276	1.90				
		342	2.36			254	1.75				
		339	2.34	Average strength		275	1.90				
		335	2.31	Average strength		268	1.85				
		311	2.15	180	457	187	1.29				
		264	1.82			176	1.21				
						Average strength		183	1.26		
				Average strength		182	1.26				
240	610			240	610	169	1.17				
						165	1.14				
						155	1.07				
		Average strength				Average strength		163	1.13		

TABLE II.- DATA ON ROOM-TEMPERATURE TENSILE STRENGTH - Continued

[Specimens are listed in order they were removed from reel]

Gage length		Ultimate stress		Gage length		Ultimate stress	
in.	cm	ksi	GN/m <sup>2</sup>	in.	cm	ksi	GN/m <sup>2</sup>
Filament A from reel 2; average strength, 386 ksi (2.66 GN/m <sup>2</sup> )				Filament A from reel 2; average strength, 386 ksi (2.66 GN/m <sup>2</sup> )			
1	2.54	232	1.60	1	2.54	346	2.39
		322	2.22			409	2.82
		353	2.44			346	2.39
		373	2.58			335	2.31
		435	2.99			405	2.80
		417	2.88			401	2.77
		397	2.74			417	2.88
		266	1.84			377	2.60
		279	1.95			294	2.03
		326	2.25			343	2.36
		302	2.08			401	2.77
		436	3.01			428	2.96
		389	2.68			255	1.76
		350	2.41			343	2.36
		409	2.82			353	2.44
		389	2.68			425	2.93
		496	3.15			417	2.88
		417	2.88			420	2.90
		436	3.01			441	3.04
		393	2.71			428	2.96
		401	2.77	Filament B			
		409	2.82	1	2.54	219	1.51
		377	2.60			236	1.63
		413	2.85			225	1.55
		385	2.66			246	1.70
		397	2.74			275	1.90
		436	3.01			270	1.86
		409	2.82			254	1.75
		361	2.42			235	1.62
		417	2.88			260	1.79
		413	2.85			284	1.96
		358	2.47	Average strength		250	1.73
		420	2.90	5	12.7	201	1.39
		441	3.04			202	1.39
		420	2.90			213	1.47
		441	3.04			230	1.59
		385	2.66			230	1.99
		343	2.36			288	1.44
		428	2.96			208	1.44
		409	2.82			225	1.55
		441	3.04			197	1.36
		436	3.01			255	1.76
		441	3.04			232	1.60
		441	3.04	Average strength		225	1.55
		405	2.80	10	25.4	190	1.31
		346	2.39			170	1.17
		277	1.91			160	1.10
		393	2.71			179	1.24
		373	2.58			204	1.41
		393	2.71			171	1.18
		397	2.74			185	1.28
		385	2.66			187	1.29
		413	2.85			164	1.13
		358	2.47			175	1.21
		425	2.93	Average strength		179	1.24
		393	2.71	15	38.1	142	0.979
		224	1.55			154	1.06
		377	2.60			134	.925
		425	2.93			164	1.13
		350	2.41			172	1.19
		275	1.90			148	1.02
		401	2.77			165	1.14
		397	2.74			131	.904
		397	2.74			131	.904
		425	2.93			179	1.24
		441	3.04	Average strength		152	1.05
		417	2.88	20	50.8	179	1.24
		381	2.63			135	.931
		361	2.42			149	1.03
		443	3.06			164	1.13
		346	2.39			125	.863
		425	2.93			116	.800
		409	2.82			117	1.01
		417	2.88			149	1.03
		433	2.99			128	.883
		389	2.68	Average strength		144	.994
		401	2.77			144	.994
		314	2.16				
		417	2.88				
		377	2.60				

TABLE II.- DATA ON ROOM-TEMPERATURE TENSILE STRENGTH - Concluded

[Specimens are listed in order they were removed from reel]

Gage length		Ultimate stress			
in.	cm	ksi	GN/m <sup>2</sup>		
Filament C; average strength, 516 ksi (3.56 GN/m <sup>2</sup> )					
1	2.54	166	1.15		
		169	1.17		
		84.3	.582		
		545	3.74		
		434	3.06		
		424	2.92		
		529	3.65		
		296	2.04		
		308	2.12		
		604	4.17		
		377	2.60		
		465	3.21		
		281	1.94		
		378	2.61		
		484	3.34		
		361	2.42		
		518	3.58		
		581	4.01		
		489	3.38		
		512	3.54		
390	2.69				
483	3.34				
520	3.59				
608	4.19				
483	3.34				
122	.842				
580	4.00				
553	3.82				
314	2.16				
Filament D; average strength, 380 ksi (2.62 GN/m <sup>2</sup> )					
1	2.54	434	2.99		
		116	.800		
		135	.932		
		360	2.48		
		549	3.78		
		472	3.26		
		458	3.16		
		520	3.59		
		510	3.52		
		520	3.59		
		Filament D; average strength, 380 ksi (2.62 GN/m <sup>2</sup> )			
		1	2.54	446	3.14
				346	2.38
				476	3.28
				507	3.50
				555	3.83
				195	1.35
				405	2.80
				270	1.86
				183	1.26
209	1.44				
219	1.51				
437	3.02				
412	3.84				
190	1.31				
327	2.26				
305	2.10				
313	2.16				
387	2.67				
552	3.81				
451	3.11				
497	3.43				
434	2.99				
458	3.16				
131	.904				
131	.904				
131	.904				
413	2.85				
180	1.24				
468	3.23				
451	3.12				
493	3.40				
360	2.48				
468	3.23				
461	3.18				
492	3.40				
309	2.13				
459	3.17				
247	1.70				
425	2.93				
495	3.42				
497	3.43				
482	3.32				
Filament E					
1	2.54	307	2.12		
		237	1.63		
		281	1.94		
		241	1.66		
		315	2.17		
		33.9	.234		
		64.0	.441		
		226	1.56		
		350	2.42		
		311	2.14		
Average strength		237	1.64		
5	12.7	282	1.95		
		203	1.40		
		188	1.30		
		222	1.53		
		62.1	.428		
		192	1.33		
		296	2.04		
		252	1.74		
		237	1.64		
		217	1.50		
Average strength		215	1.48		
10	25.4	252	1.74		
		207	1.43		
		213	1.47		
		235	1.62		
		286	1.97		
		290	2.00		
		102	.704		
		218	1.50		
		313	2.16		
		313	2.16		
Average strength		243	1.68		
15	38.1	141	.973		
		211	1.46		
		196	1.35		
		121	.835		
		198	1.37		
		176	1.22		
Average strength		176	1.22		
20	50.8	209	1.44		
		179	1.24		
		243	1.68		
		205	1.40		
		230	1.59		
		213	1.47		
Average strength		213	1.47		
72	183	155	1.07		
144	366	150	1.04		
168	426	169	1.17		

TABLE III.- DATA FROM MICROHARDNESS TESTS MADE ON POLISHED CROSS SECTIONS OF BORON FILAMENT C WITH A  $136^\circ$  (2.38 RADIANS) DIAMOND PYRAMID INDENTER UNDER A 0.1 KILOGRAM FORCE (0.98 N) LOAD

Specimen	Distance from interface, mm	DPH no.
1	0.0316	3130
	.0124	3780
	.0161	2760
	.0070	3580
	.028	4670
	.0083	3050
Core	-----	2690
2	0.0093	3480
	.026	4130
	.014	4010
	.029	3580
	.014	3780
	.029	4010
	.027	4390
	.026	3580
.030	4130	
Core	-----	2050
3	0.023	4010
	.015	3130
	.030	3580
	.016	3580

Specimen	Distance from interface, mm	DPH no.
3	0.021	2690
	.027	3050
	.016	3580
	.022	3780
Core	-----	1748
4	0.022	3480
	.020	6600
	.020	3780
Core	.028	3050
	-----	2450
5	0.025	4130
	.016	3580
	.028	3780
	.026	3480
Core	-----	2390
6	0.016	4390
	.025	4130
	.013	3780
Core	.038	3780
	-----	2900



*"The aeronautical and space activities of the United States shall be conducted so as to contribute . . . to the expansion of human knowledge of phenomena in the atmosphere and space. The Administration shall provide for the widest practicable and appropriate dissemination of information concerning its activities and the results thereof."*

—NATIONAL AERONAUTICS AND SPACE ACT OF 1958

## NASA SCIENTIFIC AND TECHNICAL PUBLICATIONS

**TECHNICAL REPORTS:** Scientific and technical information considered important, complete, and a lasting contribution to existing knowledge.

**TECHNICAL NOTES:** Information less broad in scope but nevertheless of importance as a contribution to existing knowledge.

**TECHNICAL MEMORANDUMS:** Information receiving limited distribution because of preliminary data, security classification, or other reasons.

**CONTRACTOR REPORTS:** Technical information generated in connection with a NASA contract or grant and released under NASA auspices.

**TECHNICAL TRANSLATIONS:** Information published in a foreign language considered to merit NASA distribution in English.

**TECHNICAL REPRINTS:** Information derived from NASA activities and initially published in the form of journal articles.

**SPECIAL PUBLICATIONS:** Information derived from or of value to NASA activities but not necessarily reporting the results of individual NASA-programmed scientific efforts. Publications include conference proceedings, monographs, data compilations, handbooks, sourcebooks, and special bibliographies.

*Details on the availability of these publications may be obtained from:*

SCIENTIFIC AND TECHNICAL INFORMATION DIVISION  
NATIONAL AERONAUTICS AND SPACE ADMINISTRATION  
Washington, D.C. 20546